THERMODYNAMIC AND MECHANICAL PROPERTIES OF EPON 862 WITH CURING AGENT DETDA BY MOLECULAR SIMULATION

A Thesis

by

JEREMY LEE TACK

Submitted to the Office of Graduate Studies of
Texas A&M University
in partial fulfillment of the requirements for the degree of

MASTER OF SCIENCE

December 2006

Major Subject: Chemical Engineering

THERMODYNAMIC AND MECHANICAL PROPERTIES OF EPON 862 WITH CURING AGENT DETDA BY MOLECULAR SIMULATION

A Thesis

by

JEREMY LEE TACK

Submitted to the Office of Graduate Studies of
Texas A&M University
in partial fulfillment of the requirements for the degree of

MASTER OF SCIENCE

Approved by:

Chair of Committee,	David M. Ford
Committee Members,	Tahir Cagin
	John Whitcomb
Head of Department,	N. K. Anand

December 2006

Major Subject: Chemical Engineering

ABSTRACT

Thermodynamic and Mechanical Properties of EPON 862 with Curing Agent DETDA by Molecular Simulation. (December 2006)

Jeremy Lee Tack, B.S., New Mexico State University

Chair of Advisory Committee: Dr. David M. Ford

Fully atomistic molecular dynamics (MD) simulations were used to predict the properties of EPON 862 cross-linked with curing agent DETDA, a potentially useful epoxy resin for future applications of nanocomposites. The properties of interest were density (at near-ambient pressure and temperature), glass transition temperature, bulk modulus, and shear modulus. The EPON molecular topology, degree of curing, and MD force-field were investigated as variables. The range of molecular weights explored was limited to the oligomer region, due to practical restrictions on model size. For high degrees of curing (greater than 90%), the density was found to be insensitive to the EPON molecular topology and precise value of degree of curing. Of the two force-fields that were investigated, cff91 and COMPASS, COMPASS clearly gave more accurate values for the density and moduli as compared to experiment. In fact, the density predicted by COMPASS was in excellent agreement with reported experimental values. However, the bulk and shear moduli predicted by simulation were about two times higher than the corresponding experimental values.

ACKNOWLEDGMENTS

First, I would like to extend my greatest gratitude to my thesis advisor, Dr. David M. Ford. There is no way that this thesis could have been finished without his considerable help and encouragement through my graduate study.

I am fortunate to have Dr. Tahir Cagin and Dr. John Whitcomb as committee members. Their help and suggestions have been greatly appreciated.

I would like to thank my parents, Gary Tack and Marylyn Tack, for always supporting and believing in me. Your encouragement and love made possible what I have today.

TABLE OF CONTENTS

LIST OF FIGURES

LIST OF TABLES

CHAPTER I

INTRODUCTION

There is currently great interest in the development of epoxy resin matrices for use in the composites industry. Private researchers and the US military have particular interest in using the epoxy resin Bisphenol F diglycidyl ether (EPON 862) with the curing agent DETDA for applications in nanotube composites. When EPON 862 is cross-linked with appropriate curing agents, superior mechanical, adhesive, electrical, and chemical resistance properties can be obtained [1]. However, creating nanocomposites with enhanced properties has proven challenging and there has been relatively little modeling at the nanometer scale for this particular system [2].

As a first step, we have carried out atomistic modeling of neat resins of EPON 862 with cross-linking agent DETDA, with an emphasis on predicting certain key thermodynamic and mechanical properties. This work will establish a baseline for future modeling of EPON-based nanocomposites. Molecular topology and degree of cross-linking are likely two critical parameters that determine the resin's effectiveness in staying bonded to carbon nanotubes under loading, and thus their effects on the bulk material properties are important to understand. This modeling research will complement ongoing experimental studies of the EPON-DETDA system using traditional and nanoscale characterization techniques.

This thesis follows the style of *Molecular Simulation*.

This main goal of the study is to predict certain physical and mechanical properties of EPON 862 with curing agent DETDA using molecular dynamics (MD) simulation and compare those predicted with measured values from experimentation. These properties include density, glass transition temperature, bulk modulus, shear modulus, Young's modulus, and Poisson's ratio. Another major issue is determining which MD force-fields give the most accurate property predictions as compared to experimental data. The sensitivity of the modeling predictions to assumptions about the molecular topology and degree of curing are also important to quantify.

CHAPTER II

BACKGROUND

2.1 Previous work on molecular modeling of EPON

Previous literature on this topic is very limited. A combined computational and experimental study of EPON 862 and DETDA with single walled nanotubes (SWNT) was conducted by Zhang et al. [2]. The computational work employed models of low molecular-weight cross-linked epoxy species packed around a SWNT. They performed their calculations using a set density of 1.2 g/cc and temperature of 298 K with the COMPASS force-field. They determined the interfacial bonding energy between the epoxy resin and the nanotube was .1 kcal/mol$Å^2$. Using pullout simulations they determined the interfacial shear strength of up to 75 MPa. In the experimental study they found the uniform dispersion and good interfacial bonding of the nanotubes in the epoxy resin resulted in a 250-300% increase in the storage modulus with an addition of 20-30 wt% nanotubes [2].

2.2 Molecular parameters in modeling EPON-DETDA

Before building the atomistic models, it is instructive to consider how EPON 862 and its DETDA-cured polymeric forms are synthesized. In order to form EPON 862 an epoxide is combined with Bisphenol F as seen in Figure 1. Typically the 'R' group in the epoxide is chlorine. Bisphenol F can be in three different forms ortho-ortho, para-para, and para-ortho; para-para is shown in Figure 1[3]. As a side reaction the newly formed EPON 862 can also react with Bisphenol F as seen in Figure 2, to form a long chain with an epoxide

group on each end [4]. Since the side reaction is driven by heat it can be limited. For this study the modified EPON 862 in Figure 2 is assumed to have an ‘n’ value of two.

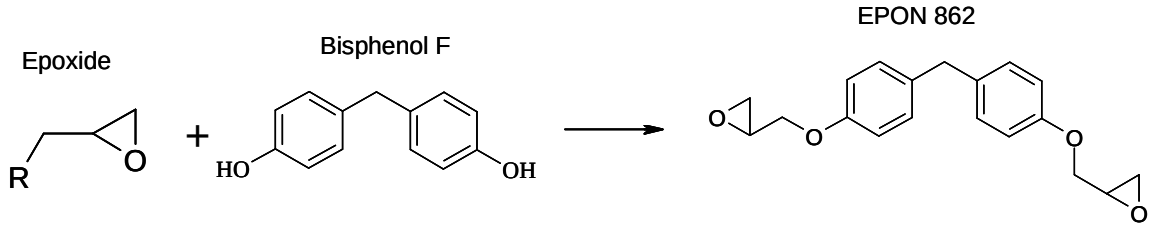

Figure 1: Formation of EPON 862

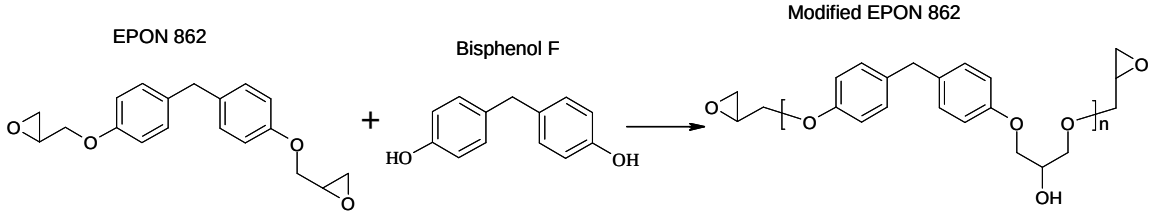

Figure 2: Addition of Bisphenol F to EPON 862

During the curing reaction of EPON 862 and DETDA the hydrogen atoms of the amine groups of DETDA react with the epoxide in EPON 862, as seen in Figure 3. The resulting molecule can then react with up to three more epoxide groups, since there are still three more hydrogen atoms left in the two amine groups. Figure 4 shows the start of the cross-linking between EPON 862 and DETDA. The molecule will continue to react with the epoxide and amine groups expanding in all directions.

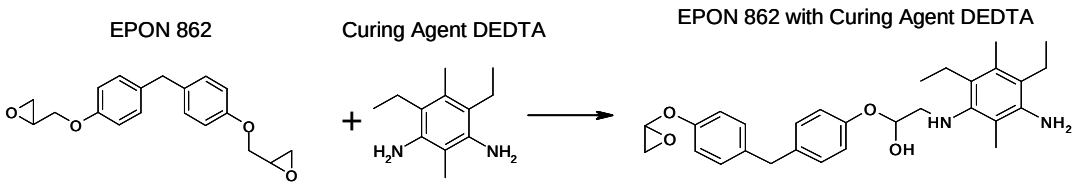

Figure 3: Reaction of EPON 862 with Curing Agent DEDTA

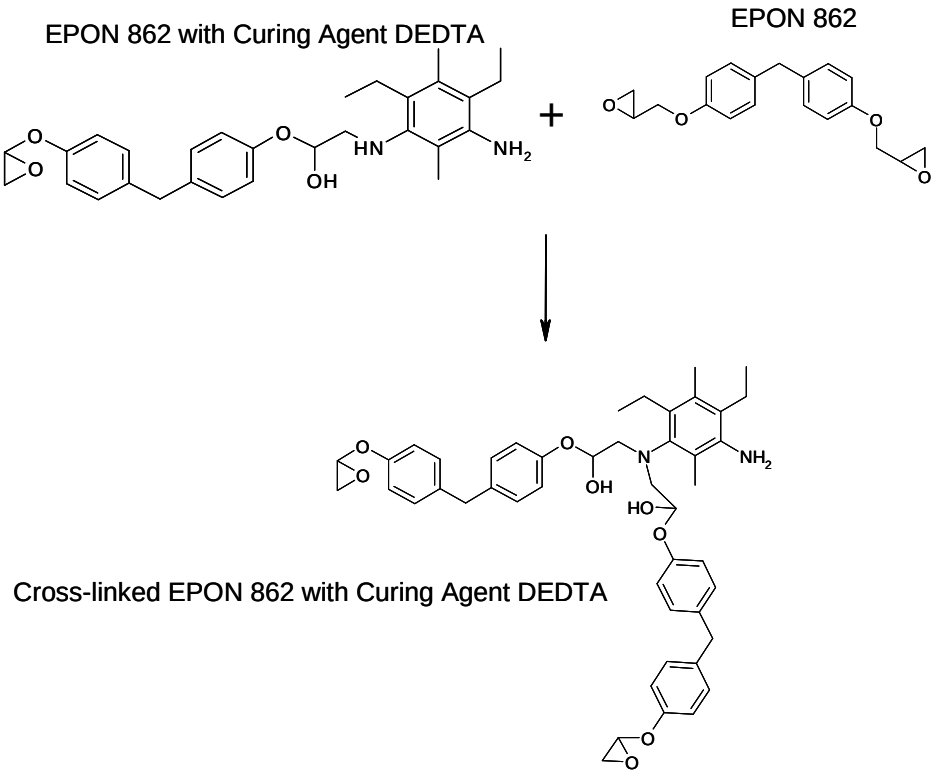

Figure 4: Start of the Cross-linking of EPON 862 and Curing Agent

In summary, when building the molecular models of cross-linked EPON 862 there are choices to be made about

(1) Ortho/para conformation of EPON monomers

(2) Extent of side reactions to produce “extended” EPON monomers (Fig 2)

(3) Degree of cross-linking with DETDA

Based on manufacturer data the ratio of EPON 862 to the curing agent is 100/26.4 by weight [5]. When forming the models the first set of models will be based on the unmodified EPON seen in Figure 1, which means that a ratio of 2.15 EPON monomers to one curing agent will be used. The next group of models will be based on the modified EPON that is formed, seen in Figure 2. For models using the modified EPON monomer the ratio of EPON to curing agent will decrease since the molecular weight of the modified EPON is higher, therefore a ratio of 2 to 1 will be used.

2.3 Molecular modeling techniques

2.3.1 *Software*

There are several software packages that are available for molecular simulation that could be used. The two that will be used in the current work are LAMMPS and Materials Studio. LAMMPS is a classical molecular dynamics (MD) code that can model systems in either a liquid, gaseous, or solid state. The code was written by Steve Plimpton and was developed at Sandia National Laboratories with funding from the Department of Energy. It is an open-source code that is freely available [6].

Materials Studio was developed by Accelrys Software Inc. The three main products of Materials Studio that will be used are Amorphous Builder, Discover, and COMPASS.

Amorphous Builder is used for building periodic cells of systems and designed especially for liquids and amorphous polymers. Discover is the MD simulation tool used in Materials Studio. COMPASS stands for Condensed-phase Optimized Molecular Potentials for Atomistic Simulation Studies. It is a force-field that is only available on Accelrys software [7].

2.3.2 *Molecular dynamics*

In classical molecular simulation, a model system is built at the atomistic level with prescribed potentials (the force-field) acting between the atoms. These interactions consist of site-site interactions, such as van der Waals dispersion and Coulombic forces, and intramolecular forces, such as chemical bonds, angle bending and dihedral torsional barriers. Models typically span on the order of 1 to 10 nm on a side, with periodic boundary conditions in one or more of the dimensions [8]. The term periodic boundary condition refers to the simulation of structures consisting of a periodic lattice of identical subunits. During the course of the simulation as a molecule moves in the original cell, its image in the other cells moves in exactly the same way[8]. Molecular and macroscopic properties of interest can be averaged over a molecular dynamics (MD) trajectory, which is simply an integration of Newton's equations of motion for all of the atoms in the system. Time spans on the order of nanoseconds may be routinely accessed with desktop computers [8,9].

An important issue in molecular dynamics simulations is the summation of the pairwise (van der Waals and Coulombic) potential functions. In principle, computing their force

contribution to the equations of motion requires $(N^2-N)/2$ terms, where N is the total number of atoms. For this study around 10,000 atoms are used for each simulation, which equates to approximately 50 million terms. Typically the problem is made tractable by splitting these forces into short-range and long-range contributions. A cut-off radius, r_{cut}, is introduced which represents an effective maximum range for the van der Waals forces. For distances that are smaller than r_{cut}, the van der Waals forces are calculated using simple summation; the limited range significantly reduces the number of pairs that must be considered. For the long-range (Coulombic) contributions, methods such as Ewald summation or particle-particle and particle-mesh (PPPM) are the common methods [10]. Ewald summation decomposes the Coulombic forces into real space and Fourier space contributions using the periodicity imposed by the boundary conditions.

In order to extract information from molecular simulations a convenient ensemble should be chosen. The two that are used in this study are NPT and NVT. NPT holds the number of atoms, pressure, and temperature of the system constant. The NVT hold the number of atoms, volume, and temperature of the system constant. The NPT ensemble is the most useful in this study since the mechanical properties are known, from experiments, at certain temperature and pressure values.

2.4 Temperature and pressure control methods

2.4.1 *Temperature control*

For controlling the temperature in a MD simulation there are four main methods velocity scale, Nose, Andersen, and Berendsen. Velocity scale controls the kinetic temperature of

a system and brings it to equilibrium by maintaining the temperature within a given range of the target temperature. When the temperature drifts outside of the specified range the atomic velocities are simply scaled back into range. Velocity rescaling method is physically unrealistic and should not be used for true temperature control. For Nose, Andersen, and Berendsen control the thermodynamic temperature and generate the correct statistical ensemble, by allowing the system to exchange energy with a heat bath [7].

2.4.2 *Pressure control*

For controlling the pressure in a MD simulation there are four main methods Parinello, Andersen, Nose and Berendsen. The Parinello method is useful for studying the stress-strain relationship in materials. Both the shape and the volume of the cell can change, which allows the internal stress of the system to match the externally applied stress. The Andersen and Nose method allows changing of the volume of the cell but keeps the shape fixed by allowing the cell to change isotropically. The Berendsen method involves changing the pressure by altering the coordinates of the particles and the size of the cell, the shape is also kept fixed [7].

2.5 Properties predicted

2.5.1. *Density*

Density at fixed temperature and pressure is a key output being measured. The density is obtained from an NPT simulation by dividing the total mass of atoms in the simulation cell by the average cell volume over the MD run.

2.5.2 *Bulk and shear moduli*

The design of this portion of the study begins with the classical equations for the shear modulus (*G*) and bulk modulus (*B*) in terms of the first and second Lamé constants λ and μ, as shown in Equations 1 and 2 respectively [11]. The shear modulus, also known as the modulus of rigidity, is the measure of elastic deformation of a body in which an applied force determines the shape of the body [12]. The bulk modulus is the ratio of the change in pressure acting on a volume to the fractional change in volume [12].

$$G = \mu \qquad \text{Eq 1}$$

$$B = \lambda + \frac{2}{3}\mu \qquad \text{Eq 2}$$

The simulations run in this study seek to find B and G in Materials Studio and use those values to find the Lamé constants λ and μ. The bulk modulus can be easily determined from Equation 3 by simply introducing a high, e.g. 5000 atm, hydrostatic pressure to the NPT simulation and observing the new average cell volume upon equilibration at this new pressure.

$$B = \frac{\Delta P}{\left(\Delta V / V_0\right)} \qquad \text{Eq 3}$$

Applying hydrostatic pressure induces no shear stress in the control volume, so it provides no information on *G*. Therefore, at this point, additional NPT simulation runs

with an induced XZ shear stress were done with each of the samples to determine *G*. A free body diagram of the loading configuration appears in Figure 5.

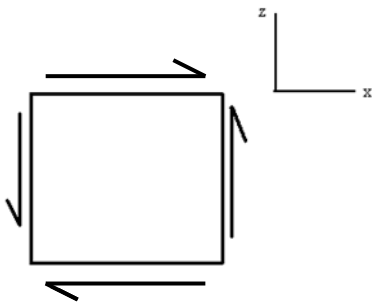

Figure 5: FBD of Loading Configuration

The method for determining the shear modulus from the data in Materials Studio takes a known value of shear stress as well as initial lattice parameters (a,b,c,α,β,γ) and looks at how the lattice deforms over time to find the shear modulus. A method for doing this calculation in free space (xyz) coordinates exists but, since the lattice parameter directions do not necessarily correspond with the x, y, and z axes, they must be arbitrarily aligned. This alignment is shown below in Figure 6 where the c direction sits aligned with the z direction, the b direction is rotated from the z axis by the lattice parameter α, and the direction is aligned off of the z axis by the angle β and the other two directions with a new angle $\bar{\gamma}$.

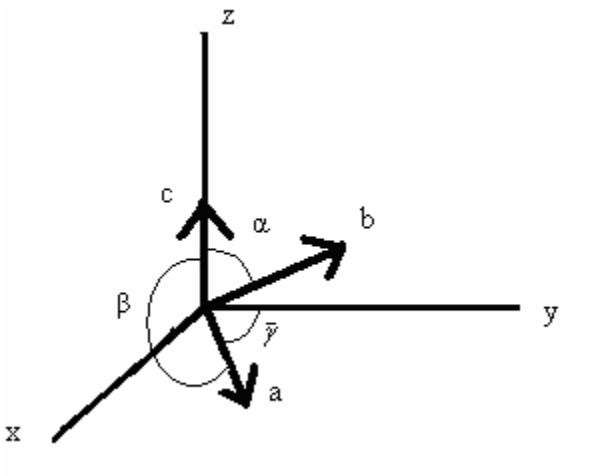

Figure 6: Alignment of Lattice Parameters

With this alignment in place, it becomes possible to convert the lattice parameters a, b, and c into the Cartesian coordinates x, y, and z with the equations in Equation 4a and 4b.

$$a_x = a*\sin\beta*\sin\bar{\gamma} \quad a_y = a*\sin\beta*\cos\bar{\gamma} \quad a_z = a*\cos\beta \quad b_x = 0 \quad c_y = 0$$

$$b_y = b*\sin(\alpha) \quad b_z = b*\cos(\alpha) \quad c_z = c \quad c_x = 0 \qquad \text{Eq 4a}$$

$$\cos\bar{\gamma} = -\frac{\cos\alpha*\cos\beta+\cos\gamma}{\sin\alpha*\sin\beta}$$

$$\sin\bar{\gamma} = \sqrt{1-\cos^2\bar{\gamma}} \qquad \text{Eq 4b}$$

These Cartesian parameters determine the lattice matrix H (Equation 5) which can be used to directly determine the 3D strain matrix from Equation 6 [13]. Shear strain in the *xz* direction can be directly taken from the strain matrix and substituted into Equation 7 along with the known shear stress to find the shear modulus.

$$H = \begin{pmatrix} a_x & b_x & c_x \\ a_y & b_y & c_y \\ a_z & b_z & c_z \end{pmatrix} \quad \text{Eq 5}$$

$$\varepsilon = \frac{1}{2}\left[{}^{T}H_0^{-1} * \left({}^{T}H * H \right) * H_0^{-1} - I \right] \quad \text{Eq 6}$$

$$G = \frac{\sigma_{xz}}{\varepsilon_{xz}} \quad \text{Eq 7}$$

Where H_0 denotes the converted lattice parameter matrix at the initial simulation conditions [14].

2.5.3 *Glass transition temperature*

The method for determining the glass transition temperature (T_g) uses density or volume data from different temperature values over a given range. Temperature is then plotted versus density. Before and after the T_g the slope of the plot should be a constant value. This allows the T_g to be determined by finding the point where the slope changes.

2.6 Run details

2.6.1 *Building the atomistic models*

Once the configuration of the EPON monomer; ortho-ortho, para-para, or para-ortho; and whether to use either the normal EPON monomer, Figure 1, or the modified EPON monomer, Figure 2, is chosen as described in section 2.2, a model is built comprising the desired number of each type of molecule packed into a simulation volume with periodic boundary conditions. For this purpose Materials Studio's Amorphous Builder package was used. Amorphous Builder inserts the molecules that you select into a periodic cell

with a density that you specify, usually lower than the target density for the system. Once the periodic cell is made the density can be adjusted by changing the periodic cell parameters in small increments, minimizing each time which prevents overlaps between atoms, until the target density is reached making sure that cell is kept in a box configuration. The system is then minimized, by optimizing the molecular structure, until the system total energy is at a minimum. Now the system is ready for dynamics to be run.

2.6.2. *Equilibration and production runs*

Now the temperature and pressure need to be stabilized before the production runs can start. Using a NVT ensemble and Berendsen temperature control the system is run for at least 20ps to stabilize the temperature at 298K. Next a NPT ensemble using Berendsen for both temperature and pressure control the system is run for another 20ps to stabilize the pressure at 1atm. Now the system is ready for production runs.

For production runs either Materials Studio or LAMMPS was used. See Table 1 for specific information on force-field and control methods used. For both programs Ewald summation will be used for long-range Coulombic forces and Van der Waal summation for short-range. See Table 2 for specific information on the adjustable parameters used. The simulations will be run for 500 ps to start with, until it is determined when equilibrium is reached, after which the total time run will be reduced, still above the time to reach equilibrium, in order to save computational time.

Starting the runs is different for each program that is used. In Materials Studio, since the models where built in this program the only thing needed is to start Discover to run them. For LAMMPS Discover is still used, but instead of running the simulation it needs to be saved to a file, making sure the correct force-field is selected. Then making use of a converter that comes with LAMMPS the file is put into the correct format for use. Since LAMMPS is a UNIX program, a script file is used to start the simulation.

Table 1: Control Methods for Software Used

	Materials Studio	**LAMMPS**
Force-field	COMPASS	Cff91
Temperature Control	Berendsen	Nose/Hoover
Pressure Control	Berendsen	Nose Hoover
Short Range Summation	van der Waals	van der Waals
Long Range Coulombic	Ewald	Ewald

Table 2: Adjustable Parameters Used for Physical and Mechanical Properties

	Temperature (K)	**Pressure (atm)**	**Shear Stress (atm)**
Density	298	1	0
Bulk Modulus	298	5000	0
Shear Modulus	298	1	100

CHAPTER III

RESULTS

3.1 Macromolecular topology/degree of curing effects on density

Starting with the assumption that just normal EPON 862 monomers and curing agent DETDA are used, without the modified EPON 862 structure seen in Figure 2, several different atomistic models were built and used with MD to predict the density at 298 K and 1 atm.

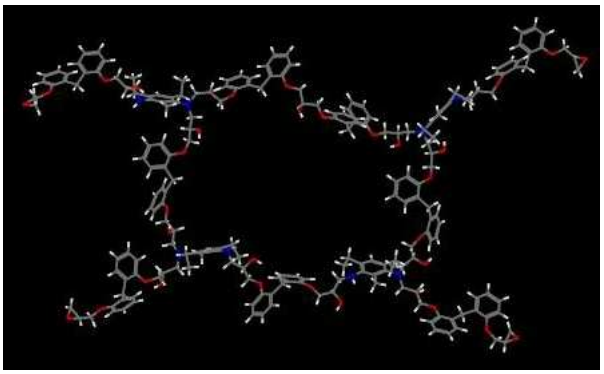

Figure 7: EPON 862 and Curing Agent Cross-Linked in a Square Configuration

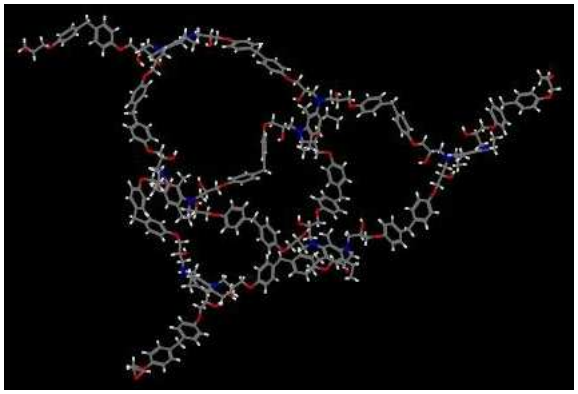

Figure 8: EPON 862 and Curing Agent Cross-Linked in a Triangle Configuration

(a) 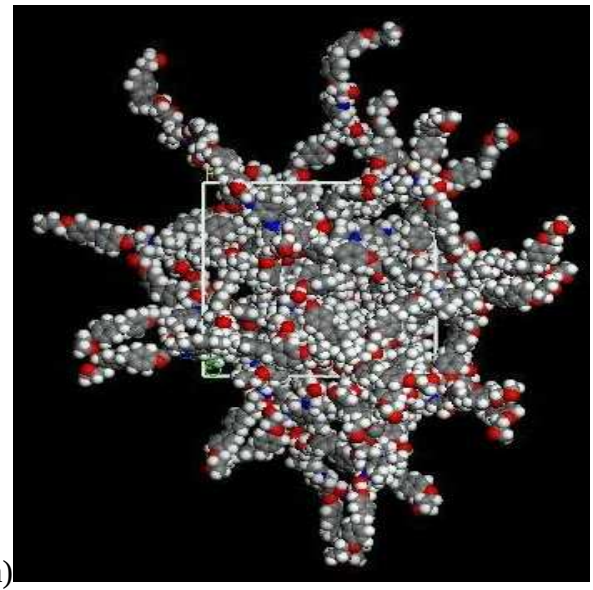 (b) 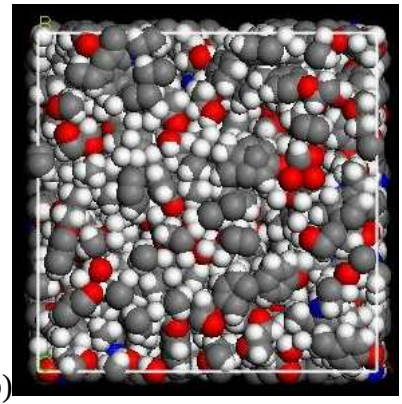

Figure 9: Two Views of Square Model System Studied. (a) Represents the default view where chemically bonded species are represented in extended form. (b) The same model that represents the periodic boundary conditions implemented where the atoms from neighboring cells are displayed.

The square, Figure 7, and triangle, Figure 8, runs both have 10 molecules, each composed of 13 EPON monomers and 6 curing agents configured in a square or triangle shape respectively. Figure 9 shows two views of the square model system, built with the Amorphous Builder software as described in section 2.6.1, where the one cell representation, (b), shows an almost uniform distribution of atoms filling the simulation cell of an amorphous system. Since the individual molecules (Figures 7 and 8) are somewhat two-dimensional by construction, one concern is that the final packed models (Figure 9) might have unrealistic structural anisotropies (although the techniques of Amorphous Builder are designed to maximize the isotropy). From visual inspection of the packed models, using representations like Figure 9 and also the free-volume

visualization tool in Materials Studio, there was no obvious indication of anisotropic conditions. However, this does not guarantee that some level of anisotropy is not present.

The partially cured run has 9 molecules, each composed of 13 EPON monomers and 6 curing agents in a square configuration and 13 EPON monomers and 6 curing agent molecules that are not bonded to each other, which corresponded to a 90 percent cured sample. The liquid run was a set of EPON monomers and curing agents that are not bonded to each other. Table 3 summarizes the data.

Table 3: Comparison of Density for Different Model Configurations

	cured90	liquid	square	triangle
Density Range	1.061-1.078	1.002-1.024	1.036-1.061	1.018-1.049
Average	1.067	1.011	1.054	1.039
Standard Deviation	0.0088	0.0085	0.012	0.014
Time (ps)	600	1000	600	900
Number of runs	5	5	4	4

These four models show that the molecular topology and degree of curing (above 90%) does not have a statistically significant effect on the density. On the other hand, a completely unbonded, (liquid) model does predict a significant lower density. Since the molecular topology does not have a significant effect, the square configuration will be used for the rest of the tests. All of these run also showed that they where at equilibrium before 75 ps, therefore to reduce computer time the rest of the runs will be run for 100 ps.

Since it is known that EPON 862 can have a modified structure as seen in Figure 2, another set of atomistic models were built using the modified structure. All runs were obtained with LAMMPS using the force-field cff91 at 298K and 1 atm.

The modified runs have 10 molecules, each composed of 7 normal EPON monomers and 1 modified EPON monomers and 4 curing agents configured in a square. The modified cured run has 9 molecules, each composed of 7 normal EPON monomers and 1 modified EPON monomers and 4 curing agents configured in a square and 7 normal EPON monomers and 1 modified EPON monomer and 4 curing agent molecules that are not bonded to each other. Half of the models used the ortho-ortho configuration for EPON 862 and the other used the para-para configuration. Experimental data from manufacture web site [5]. Table 4 summarizes the data.

Changing to the modified EPON monomer led to only a two percent increase in the density. Whereas changing the configuration from ortho-ortho to para-para did not significantly change the range of density values.

Table 4: Comparison of Different Configurations of EPON 862

	Ortho-Ortho	Para-Para	Cured	Experimental
Density Range	1.054-1.082	1.058-1.083	1.068-1.074	1.17-1.2
Average	1.073	1.075	1.07	
Standard Deviation	0.0114	0.0105	0.0028	
Time (ps)	100	100	100	
Number of runs	5	5	3	

3.2 Force-field effects on density

The quality of the force-field that is applied in MD simulations is critical to the accuracy of the predications. In addition to the cff91 force-field, the COMPASS force-field was also evaluated. The force-field cff91 is freely available and transferable to any MD simulation software, unlike COMPASS which is proprietary to Accelrys Inc and can only be run on their software (e.g. Materials Studio or Cerius^2).

Due to the fact that Materials Studio is run on a PC environment, this limits the size of the model and how fast it runs. All runs on Materials Studio were reduced from 10 molecules to 5, but otherwise where the same as the modified runs using LAMMPS. Experimental data are from the manufacturer's web site [5]. Table 5 summarizes the data.

Table 5: Comparison of Density for Different Force-fields

	Cff91	COMPASS	Experimental
Density Range	1.054-1.082	1.123-1.1345	1.17-1.2
Average	1.074	1.13	
Standard Deviation	0.0104	0.0061	

From Table 4 it is clear that by changing the force-field the density has increased by over five percent. This shows that the force-field has a significant effect on the model that is being used. The density is now 3-6% lower than the experimental values using COMPASS versus 8-11% lower with cff91.

3.3 Mechanical properties

First, the bulk modulus test was run using an NPT ensemble with temperature set to 298K and pressure set to equilibrate at 5000 atm. The equilibrating pressure changes the volume of the periodic cell by an amount equal to ΔV in Equation 3. Knowing how the pressure changed and the initial and final dimensions of the control volume, the bulk modulus can be calculated. Experimental bulk modulus data is from the research group of D. Lagoudas [15]. Table 6 summarizes the results.

Table 6: Comparison of Bulk Modulus for Different Force-fields

	Cff91	COMPASS	Experimental
Bulk Modulus(GPa) Range	5.64-6.036	4.84-5.54	
Average	5.79	5.18	2.9
Standard Deviation	0.213	0.535	

It is clear that the COMPASS force-field estimates that bulk modulus better than cff91 does, but both are clearly higher, 1.5-2x, than the experimental value. This is because the simulation system represents an ideal system, whereas the experimental system may have microscopic or even macroscopic defects. So the simulated values can be seen as the upper limit on what the value can be [16].

Next, the shear test was run using another NPT ensemble with temperature of 298K. Pressure control is the key factor is this run. The pressure was set to one atm, but a shear stress of 100 atm was added in the XZ cell direction and Parinello barostat control was used. The change to a Parinello control system for pressure was due to the fact that

Berendsen control keeps the lattice in the original cubic shape, but to calculate the shear modulus the lattice shape needs to be able to change with the shear. The ensemble provides the lattice parameter values necessary in the calculation described in section 2.5.2. Occasionally when running the system with a shear stress it was noted that erroneous results were received. On average the erroneous results occurred in about ten percent of the runs conducted. The usual result was that the system would not run to completion, i.e. the system would crash. Occasionally the results would be an unrealistic result, usually extremely high or a negative number. The extremely high results usually were caused when the system would be on the verge of crashing, but the run finished before this happened causing the values reported to be very high.

With the values of B and G known, calculation of the Lamé constants as well as Poisson's ratio(ν) and Young's modulus (E) became possible using Equations 1 and 2 above as well as the two equations below in Equation 8[11]. Poisson's ratio is the ratio of transverse contraction strain to longitudinal extension strain in the direction of stretching force [17]. Young's modulus is a measure of the stiffness of a given material. It is defined as the ratio, for small strains, of the rate of change of stress with strain [18].

$$E = \mu\frac{3\lambda + 2\mu}{\lambda + \mu} \qquad \nu = \frac{\lambda}{2(\lambda + \mu)} \qquad \text{Eq 8}$$

From experiments in the research group of D. Lagoudas, the bulk, storage (E'), and loss (E'') moduli are known [15] see Table 7.

Table 7: Experimental Values of Storage and Loss Modulus

	Experimental		Calculated
	Storage (E')	Loss (E'')	Young's (E)
Sample 1	2.843	0.21	2.85
Sample 2	2.913	0.223	2.92
Sample 3	1.908	0.113	1.91
Average	2.555	0.182	2.59
Standard Deviation	0.561	0.0601	0.564

The Young's modulus can be calculated from the storage and loss modulus, see Table 7, by using Equation 9 [19]. Having the Bulk and Young's modulus allows the calculation of the shear modulus and Poisson's ratio.

$$E = E' + iE'' \qquad |E| = \sqrt{(E')^2 + (E'')^2} \qquad \text{Eq 9}$$

Final calculated values are presented below in Table 8.

Table 8: Comparison of Mechanical Properties

	λ(GPa)	μ(GPa)	Bulk(GPa)	Shear(GPa)	Young's(GPa)	Poisson
COMPASS	4.81	.557	5.18	.557	1.61	.448
Experimental	2.27	.946	2.9	.946	2.56	.353

The reason that only COMPASS results are shown is that LAMMPS is unable to predict the shear modulus using the method described above.

3.4 Glass transition temperature

The glass transition temperature (T_g) can be obtained by generating density data at different temperatures and looking for a change in the slope of a density vs. temperature plot [20,21]. See Figure 10

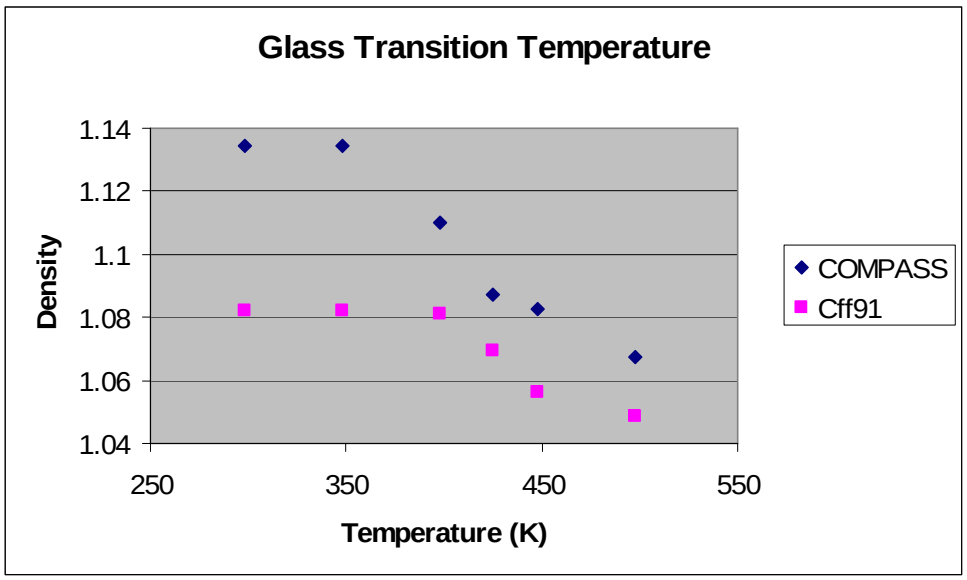

Figure 10: Plot of Density vs. Temperature

By looking at Figure 10 the T_g can be seen to be between 350 and 400K for COMPASS and between 400 and 425K for cff91. Experimentally the value of T_g have been reported, by the research groups of D. Lagoudas and H. J. Sue, between 418 and 434K [15,22]. From this it seems that for estimating the T_g, the cff91 force-field is the better choice.

CHAPTER IV

CONCLUSIONS

This study of EPON 862 with curing agent DETDA using molecular dynamics simulation focused on three main points: predict key physical and mechanical properties; evaluate the effects of molecular topology on the predictions; and determine which type of force-field gives the most realistic results as compared to experiment.

The physical and mechanical properties that were predicted and compared with experimental values were density, glass transition temperature, bulk modulus, shear modulus, Young's modulus, and Poisson's ratio. In the best cases, the predicted density was within 6% of the experimental value and the predicted T_g was within 3%. The modulus is where molecular dynamics has a problem predicting the values. The calculated bulk modulus was at least 1.5 times higher than the experimental value. This is because the simulated system represents an ideal system, whereas the experimental may have microscopic or even macroscopic defects. The Young's modulus was about 0.6 times the experimental value and Poisson's ratio was about 1.3 times higher than the experimental value. The reasons that the Young's modulus is lower than the experimental value are likely (1) slightly non-isotropic systems and (2) the models being used are smaller than those used experimentally.

For the molecular topology effects, the ortho/para conformation, degree of cross-linking with DETDA, and the extent of side reactions were examined. EPON 862 can be in

ortho-ortho, para-para, or para-ortho types of conformation. It was found that the type of conformation had no statistical impact on the predicted density of EPON at near-ambient conditions. The amount of cross-linking directly impacts the physical properties. Samples with no cross-linking, where none of the molecules are bonded to each other, were compared to oligomeric, i.e. a polymer with only a few monomers, samples with cross-linking based on manufacturer data; a 5-6% increase in the density with cross-linking was observed using the cff91 force-field. For the cross-linked samples, the particular configuration of the oligomers had little impact on the predicted density. The side reaction, which added an extra Bisphenol F group to EPON 862, showed only a slight increase in the density, about 2%. Overall the aspect of molecular topology that most affected the physical properties was the amount of cross-linking.

Two force-fields were evaluated during this study: cff91 using LAMMPS, and COMPASS using Materials Studio. The cff91 force-field was found to be more effective only in calculating the glass transition temperature. For everything else COMPASS was more accurate, as judged by comparison with experimental data. The drawback of using COMPASS is that it is proprietary to Accelrys, whereas cff91 can be used with any software package.

CHAPTER V

FUTURE WORK

Since the mechanical properties that are being calculated are not matching what is being found experimental something needs to be done. Due to the fact that the force-field employed is critical to the accuracy of the predictions of the simulations, better force-fields need to be found. One thing that can be done is to develop a new force-field from scratch that predicts the mechanical properties more accurately. Additionally existing force-fields could be modified. While this should bring the mechanical properties closer to the experimental values it will not solve all the problems.

Microscopic and/or macroscopic defect could also be affecting the mechanical properties. Microscopic defects could be included in the current models that are being used, but not knowing what type of defects, and how many, that could be found in this system limit the testing capabilities. Macroscopic defects cannot be tested in our models since the defect would be as large as the total model. Macroscopic defects would need to be tested using mesoscale dynamics. A way to bridge molecular and mesoscale dynamics needs to found in order for the full effects of defects to be tested.

Now that the structural behavior and the mechanical properties are known, the next step in this project is to start adding nanotubes into the molecular simulation. The nanotube should be surrounded by cross-linked EPON 862 with DETDA. Several problems arise when doing this. First is since Amorphous Builder in Materials Studio inserts molecules

randomly into a periodic cell the nanotube might not be where it should be. Therefore several iterations will be necessary until the nanotube is positioned correctly. Once the nanotube is in the correct position, normal molecular dynamics will not be a problem until high pressure is added to the system. Due to the cylindrical structure of nanotubes problems arise when adding high pressure to the system, for calculation of the Bulk modulus. When the nanotube is compressed it tends loss its cylindrical shape, when using the COMPASS force-field. Other force-fields might not have this same problem and needs to be looked into. A method will need to be developed, using current force-fields to make sure that the nanotubes retain their shape but still allow for heavy compression of around 5000 atm. Adding a shear stress to the system might cause the same type of problem and will need to be looked into.

Once the solutions to these problems have been solved additional nanotubes will be added one at a time to the system until they no longer give a significant increase to the mechanical and structural properties of the system. Knowing the upper limit on the number of nanotubes that can be added to the system will allow cost versus impact projections to be made. Once the optimum number of nanotubes to be added to the system is known, it will give the experimentalists a good starting point for their testing.

REFERENCES

[1] http://www.hexionchem.com/pds/E/EPON%20Resin%20862.pdf; Product bulletin EPON Resin 862; Resolution Performance Products (2005)

[2] Jihua Gou, Bob Minaie, Ben Wang, Zhiyong Liang, Chuck Zhang; Computational and Experimental Study of Interfacial Bonding of Single-walled Nanotube Reinforced Composites; *Computational Materials Science*, **31**, 225-236 (2004)

[3] http://www.sigmaaldrich.com/catalog/search/ProductDetail/FLUKA/15144; Bisphenol F diglycidyl ether; Sigma-Aldrich; Accessed May 2006

[4] Minoru Kobayashi, Fumio Sanda, and Takeshi Endo; Application of Phosphonium Ylides to Latent Catalysts for Polyaddition of Bisphenol A Diglycidyl Ether with Bisphenol A: Model System of Epoxy-Novolac Resin; *Macromolecules*, **32** (15), 4751 - 4756 (1999)

[5] http://www.hexionchem.com/pds/E/EPIKOTE™%20Resin%20862%20EPIKURE™%20Curing%20Agent%20W.pdf; Product bulletin EPIKOTE Resin 862/ EPIKURE Curing Agent W System; Resolution Performance Products, (2001)

[6] http://lammps.sandia.gov/doc/Manual.html, LAMMPS Documentation; Steve Plimpton, Paul Crozier, and Aidan Thompson (2006)

[7] http://www.accelrys.com/products/mstudio; Materials Studio; Accelrys (2006)

[8] M.P. Allen and D.J. Tildesley; *Computer Simulation of Liquids*; Oxford Science Publications; New York, (1987)

[9] Daan Frenkel and Berend Smit; *Understanding Molecular Simulation From Algorithms to Applications*; Academic Press; San Diego, CA (2002)

[10] W.K. Liu, E.G. Karpov, S. Zhang, H.S. Park; An Introduction to Computational Nanomechanics and Materials; *Computer Methods in Applied Mechanics and Engineering*, **193** 1529-1578 (2004)

[11] Doros N. Theodorou and Ulrich W. Suter; Atomistic Modeling of Mechanical Properties of Polymeric Glasses; *Macromolecul*es, **19**, 139-154 (1986)

[12] http://www.grantadesign.com/resources/materials/glossary.htm; Glossary of Materials Attributes; Granta Design Limited (2006)

[13]); A.M. Kosevich, E. M. Lifshitz, L. D. Landau, L. P. Pitaevskii; *Theory of Elasticity, Third Edition: Volume 7 (Theoretical Physics, Vol 7)*; Pergamon Press; Oxford, NY (1986)

[14] Tahir Cagin, 241 Jack E. Brown Engineering Building, Personal Communication

[15] Dimitris Lagoudas, 736A H.R. Bright Building, Personal Communication

[16] Cun Feng Fan, Tahir Cagin, and Zhuo Min Chen; Molecular Modeling of Polycarbonate. 1. Force Field, Static Structure, and Mechanical Properties; *Macromolecules*, **27**, 2383-2391 (1994)

[17] http://silver.neep.wisc.edu/~lakes/PoissonIntro.html; Meaning of Poisson's ratio; Rod Lakes; Accessed Aug 2006

[18] http://www.answers.com/topic/young-s-modulus; Young's modulus; Answers Corporation (2006)

[19] S J Bull; Nanoindentation of Coatings; *Journal of Physics D: Applied Physics*, **38**, R393-R413 (2005)

[20] Taining Liang, Yong Yang, Dawei Guo, and Xiaozhen Yang; Conformational Transition Behavior Around Glass Transition Temperature; *Journal of Chemical Physics*, **22**, v112, n4 2016-2020 (2000)

[21] Jie Han, Richard H. Gee, and Richard H. Boyd; Glass Transition Temperatures of Polymers from Molecular Dynamics Simulations; *Macromolecules*, **27**, 7781-7784 (1994)

[22] Hung-Jue Sue, 215 Engineering/Physics Building Office Wing, Personal Communication

VITA

Name:	Jeremy Lee Tack
Address:	P.O. Box 866, Corrales, NM
Email Address:	jtack13@yahoo.com
Education:	M.S., Chemical Engineering, Texas A&M University, 2006
	B.S., Chemical Engineering, New Mexico State University, 1997